Theory of unpinning of spiral waves using circularly polarized electric fields in mathematical models of excitable media

Shreyas Punacha, Naveena Kumara A., and T. K. Shajahan
Department of Physics, National Institute of Technology Karnataka Surathkal, Mangalore, Karnataka, 575025, India

(Received 20 March 2020; accepted 31 August 2020; published 21 September 2020)

Spiral waves of excitation are common in many physical, chemical, and biological systems. In physiological systems like the heart, such waves can lead to cardiac arrhythmias and need to be eliminated. Spiral waves anchor to heterogeneities in the excitable medium, and to eliminate them they need to be unpinned first. Several groups focused on developing strategies to unpin such pinned waves using electric shocks, pulsed electric fields, and recently, circularly polarized electric fields (CPEF). It was shown that in many situations, CPEF is more efficient at unpinning the wave compared to other existing methods. Here, we study how the circularly polarized field acts on the pinned spiral waves and unpins it. We show that the termination always happens within the first rotation of the electric field. For a given obstacle size, there exists a threshold time period of the CPEF below which the spiral can always be terminated. Our analytical formulation accurately predicts this threshold and explains the absence of the traditional unpinning window with the CPEF. We hope our theoretical work will stimulate further experimental studies about CPEF and low energy methods to eliminate spiral waves.

DOI: 10.1103/PhysRevE.102.032411

I. INTRODUCTION

Spiral waves have been found in a variety of human organs like the surface of the retina causing migraine [1], inside the brain fostering epilepsy [2], and in the heart muscle leading to fatal cardiac arrhythmias [3]. Spiral waves thrive in a class of media whose individual components are interconnected by diffusion-like coupling. In such a medium, a perturbation that exceeds a threshold will induce an excitation wave, which gets propagated among the individual components across the medium. In many physiological tissues, such rotating waves of activity are pathological, and in the heart, it leads to cardiac rhythm disorders or even fatal conditions such as ventricular fibrillation [4]. Thus in many situations, it is desirable to remove such spiral waves from the medium. However, in heterogeneous media, rotating spiral waves tend to move towards heterogeneities (henceforth called obstacles) in the medium and rotate around the boundary of the obstacle as if the wave is pinned to it.

Unpinning a pinned wave requires a careful stimulus given close to the core of the pinned wave and within a short time interval known as the unpinning window of the spiral wave [5]. This is often not practical since there can be many obstacles in a physiological tissue, which can pin the spiral. Pumir and Krinsky [6] showed that if we apply an electric field across the tissue, it can generate secondary excitations from the boundary of the obstacles which can act as a local stimulus close to the core of the pinned wave. This method, known as far-field pacing (FFP), eliminates the problem of locating the stimulus, instead it allows one to time these field pulses so that the secondary excitations are within the unpinning window of the wave [7,8]. This method was successfully applied to control such waves in the heart during fibrillation [9].

Jiang-Xing Chen *et al.* introduced the circularly polarized electric field (CPEF) to study its influence on the drift of the spiral waves [10]. Later, Feng *et al.* used it to terminate the pinned spiral waves [11]. In a simulation study, they compared the efficiency of the circularly polarized electric field to that of the pulsed electric field and found a significant increase in the success rate with much lower voltage strength than pulsed electric fields. In the subsequent study, they showed that the higher frequency circular wave trains generated by the CPEF could successfully terminate spiral turbulence [12]. Recently, the effect of CPEF on an irregularly shaped obstacle was also performed [13]. In addition to these studies, the ability of CPEF to control the turbulence has been shown experimentally in the Belousov-Zhabotinsky reaction [14].

In this article, we present a mechanism for unpinning the spiral waves using CPEFs. We show that, for a given obstacle size, there exists a time period of the CPEF below which the spiral can always be unpinned. We call it the cutoff time period. We also show that the termination always happens within the first period of the CPEF. In the following sections, first, we summarize the observations made in the simulations. Later, based on these observations, we derive a robust and generalized analytical formulation which explains the findings of the simulations. Our theory accurately predicts the cutoff time period of CPEF. In particular, we show that unpinning is always successful if the period of the CPEF is below the cutoff period. We also show that the cutoff period depends linearly on the radius of the obstacle. We find that there is no traditional unpinning window with the CPEF.

II. MATHEMATICAL MODEL

To simulate CPEF we use a generic model of excitation waves, namely, the Fitzhugh-Nagumo equations. They are

given by

$$\frac{\partial u}{\partial t} = \frac{1}{\epsilon}(u(1-u)(u-a) - v) + D\nabla^2 u, \tag{1}$$

$$\frac{\partial v}{\partial t} = bu - v, \tag{2}$$

where u is the transmembrane voltage and v is the slow variable. The parameter ϵ is the ratio of timescales between u and v and D is the diffusion coefficient. The equations are solved using the forward Euler scheme in time and five-point finite difference stencil on a two-dimensional (2D) square grid. The domain boundaries are modelled using no-flux boundary conditions. In monodomain models, an additional no-flux boundary condition is applied on the boundary of the obstacle to simulate the wave emission from heterogeneity. It is given by [15–17],

$$\hat{n} \cdot (D\nabla u - \boldsymbol{E}) = 0. \tag{3}$$

Here $\boldsymbol{E}$ is the applied electric field. The boundary conditions are imposed on the obstacle using the phase field method [17,18]. This method substitutes Eq. (3) by evolving an auxiliary phase field which behaves like an order parameter at the boundary of the obstacle. For $\boldsymbol{E}$, we used an anticlockwise rotating CPEF of the form $\boldsymbol{E} = E_0 \sin(2\pi t/T_{cp})\hat{x} + E_0 \cos(2\pi t/T_{cp})\hat{y}$, where E_0 is the strength of the field and T_{cp} is its period.

The parameter values are chosen as $a = 0.1$, $b = 0.25$, $\epsilon = 0.025$, $D = 1$, and $E_0 = 0.1$. We used dimensionless space step $dx = 0.1$ and time step $dt = 0.0001$. Spiral waves rotating anticlockwise were initiated in the medium with their tips pinned to the obstacles. Since we have the freedom of applying the $\boldsymbol{E}$ field either in the clockwise or anticlockwise direction, in this article, we consider anticlockwise rotating spirals only (The case of the clockwise rotating spiral is included in the Appendix). We define the phase difference α as the angular difference between the spiral and the initial direction of the $\boldsymbol{E}$ field. The waves were allowed to perform at least four rotations before the delivery of the $\boldsymbol{E}$ field.

III. RESULTS AND DISCUSSION

A. Numerical studies of unpinning with circularly polarized electric field

Figure 1 shows the unpinning of the anticlockwise rotating spiral by a CPEF. The spiral is pinned to an obstacle of fixed radius $r = 4$. The period of the spiral T_s around this obstacle is 12.5. In Figs. 1(a) to 1(d), the CPEF having a period $T_{cp} = 10.4166$ is used. Figure 1(a) shows the spiral S with $\alpha = 0$. When $\boldsymbol{E}$ field is applied, the wave emission happens from those points on the obstacle boundary where the field density is sufficient to nucleate a new wave. This gives rise to symmetrical crescent-shaped depolarization, which can be divided into head H and tail T. The head H follows the electric field vector along the boundary of the obstacle. When T collides with S, H lags behind S by a phase angle of ϕ. Due to this, H continues to stay pinned to the obstacle. In Figs. 1(e) and 1(f), the $\boldsymbol{E}$ field having a period $T_{cp} = 3.6764$ is used. Since the radius of the obstacle is fixed and T_{cp} is shorter than in the case of Figs. 1(a) to 1(d), H moves faster on the boundary and reaches the wave back of S when T and

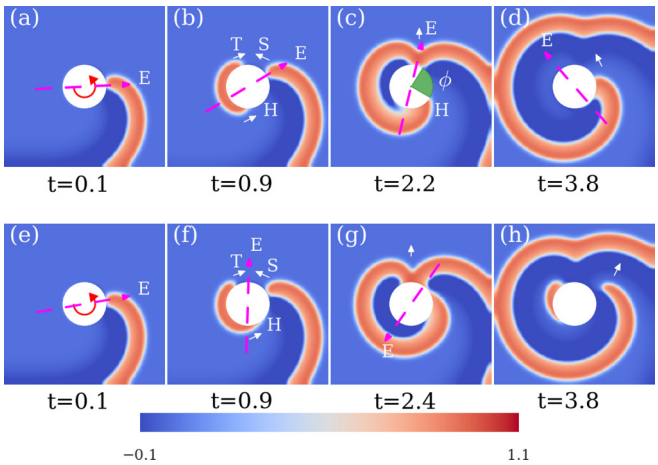

FIG. 1. Unpinning of anticlockwise rotating spiral. The radius of the obstacle (white circular patch), $r = 4$ and the phase difference $\alpha = 0$. (a)–(d) Unsuccessful case, period of the CPEF $T_{cp} = 10.4166$. (a) An anticlockwise rotating pinned spiral wave S. (b) Excitation is emitted from the obstacle. The leading end, labeled as head H, follows the electric field. The trailing end is labeled as the tail T. (c) T collides with S. The excitable gap $\phi > 0$ (shaded in green) between H and the wave back of S do not facilitate unpinning. (e)–(h) Successful case. The electric field now has a smaller period $T_{cp} = 3.6764$. (g) When T collides with S, H reaches the wave back of S. The excitable gap is zero, and this leads to successful unpinning (h). Notations: Magenta dashed arrows show the instantaneous direction and red circular arrows within the obstacle show the direction of rotation of the electric field.

S collide. This makes the phase width $\phi = 0$ and causes a successful unpinning of the spiral.

Since we kept the radius of the obstacle and phase difference α fixed, if we keep on reducing the time period T_{cp}, we must reach a point where the excitable gap $\phi = 0$. This is the cutoff time period T^*_{cp} of the $\boldsymbol{E}$ field. Below this, ϕ is always zero, and therefore there is always unpinning.

What happens if we continue to apply the $\boldsymbol{E}$ field in the unsuccessful case of Figs. 1 (a) to 1(d)? Will the spiral unpin if we apply multiple rotations of $\boldsymbol{E}$ field by keeping the value of T_{cp} fixed? In Figs. 1(a) to 1(d) $T_{cp} < T_s$. So, the head H is being dragged along by the electric field vector along the boundary of the obstacle. Due to this, the tail of the electric field vector, around which, the wave nucleation happens, always stays behind H [see Fig. 1(d)]. Since H leaves a refractory tail behind it as it moves, the electric field is not able to nucleate any waves there. So, when $T_{cp} < T_s$, applying multiple rotations of the $\boldsymbol{E}$ field do not unpin the spiral wave.

The case with $T_{cp} > T_s$ is shown in Fig. 2. Here, every time the $\boldsymbol{E}$ field nucleates a new wave, the head H of the newly nucleated wave moves with the same speed as that of the spiral instead of the speed dictated by the applied $\boldsymbol{E}$ field. Since the period of the $\boldsymbol{E}$ field is high compared to the period of the spiral, the electric field keeps lagging behind the spiral. As the $\boldsymbol{E}$ field lags and falls out of the refractory tail of H, it nucleates a new wave there. Because all the pinned waves now move with the same velocity on the boundary of the obstacle, the head H of the newly nucleated wave cannot catch up with the previous one. Therefore, the excitable gap ϕ can never

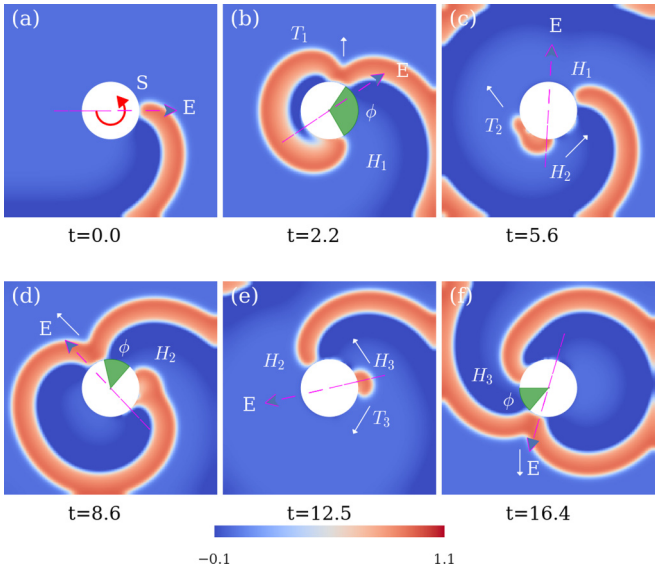

FIG. 2. Unpinning failure when $T_{cp} > T_s$. The radius of the obstacle is $r = 4$ and the phase difference $\alpha = 0$. The period of the E field is $T_{cp} = 23.22$ and the period of the spiral $T_s = 12.5$. Here, the newly nucleated heads H_1, H_2, and H_3 move with the same period as that of the spiral. (a) A pinned anticlockwise spiral S. (b) When S and T_1 collide, the excitable gap ϕ (shaded in green) is nonzero. This leads to failure of unpinning. (c) The E field falls behind the refractory tail of H_1 and nucleates a new wave with head H_2 and tail T_2. (d) When T_2 collides with H_1 the nonzero ϕ leads to failure of unpinning. (e) The E field lags once again and nucleates a new head H_3 and tail T_3. (f) The unpinning fails in a similar fashion, as shown in (d).

vanish [Figs. 2(d) and 2(f)]. So, if the unpinning fails within the first rotation of the $\boldsymbol{E}$ field, then it keeps failing irrespective of whether T_{cp} is lesser or greater than T_s.

B. Theory of unpinning with circularly polarized electric field

To provide validation for the unpinning mechanisms observed in the simulations, we derive analytical formulas based on the following assumptions. Figure 3 shows the schematic diagram of the anticlockwise spiral unpinning. On the application of the $\boldsymbol{E}$ field at $t = 0$, the wave nucleates from an extended region rather than a point. At time t_0, just after the

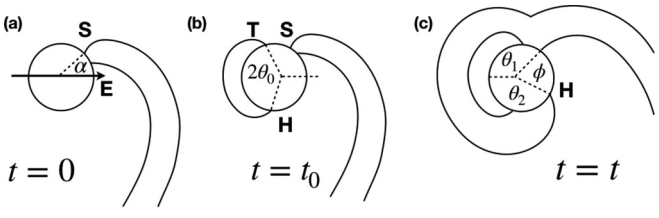

FIG. 3. Schematic diagram of anticlockwise spiral unpinning. (a) Pinned spiral wave, S at time $t = 0$. α is the angular difference between the $\boldsymbol{E}$ field and the spiral wavefront at time $t = 0$. (b) At $t = t_0$, excitation emerges out symmetrically making an angle θ_0. Meanwhile, S covers a distance of $v_s t_0$. (c) S and T collide at time t. θ_1 and θ_2 are the angle covered by T and H. The excitable gap $\phi = 2\pi - (\theta_1 + \theta_2)$.

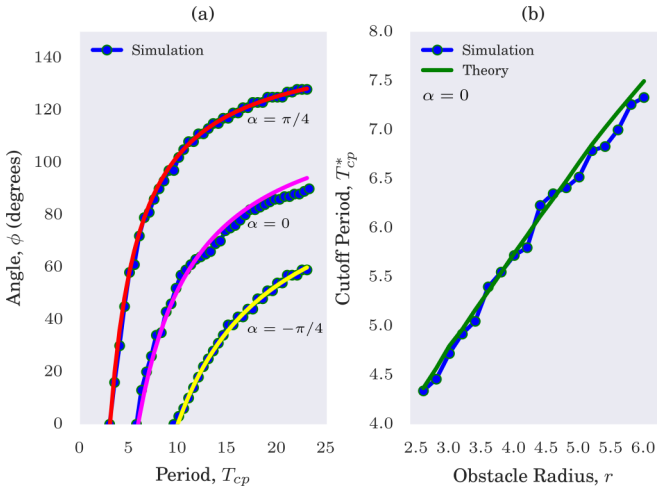

FIG. 4. (a) Graph of the excitable gap ϕ as a function of period of the circularly polarized electric field T_{cp} for anticlockwise rotating spiral. The radius of the obstacle $r = 4$. α's denote the phase difference between the spiral and the initial direction of the electric field. The solid lines represent the theoretical curves. (b) Graph of cutoff period T^*_{cp} as a function of obstacle radius r for anticlockwise rotating spiral. The value of $\alpha = 0$.

wave emerges and before it starts moving, it subtends an symmetric angle of $2\theta_0$. In the time it takes for the wave to emerge from the obstacle, the spiral S would move a distance of $r\alpha + v_s t_0$ in the anticlockwise direction. Here, $v_s = (2\pi r/T_s)$ is the velocity of S. Eventually, T and S collide. The expression for the collision time t between T and S can be obtained as follows. The angular distance covered by S in an anticlockwise direction in time t can be expressed as $\alpha + (v_s t)/r$. At the same instant, T collides with S traveling clockwise and covering an angle $\theta_1 = \theta_0 + [v_T(t - t_0)]/r$, where, v_T is the velocity of T. But we have $[\theta_1 + \alpha + (v_s t)/r] = \pi$. So, we can write the expression for t as follows:

$$t = \frac{r}{v_s + v_T}\left(\pi - \alpha - \theta_0 + \frac{v_T t_0}{r}\right). \tag{4}$$

Meanwhile, H moves an angle of $\theta_2 = \theta_0 + (2\pi/T_{cp})(t - t_0)$ in the anticlockwise direction. But the total angle is $\theta_1 + \theta_2 + \phi = 2\pi$. Therefore, the final expression for the excitable gap ϕ can be written as

$$\phi = \pi + \alpha + \frac{v_s t}{r} - \theta_0 - \frac{2\pi}{T_{cp}}(t - t_0) - \theta_{sw}. \tag{5}$$

In Fig. 3(c), we considered ϕ as the angle between the wavefront of H and the waveback of S. However, on deriving the equation, we found that the value of ϕ measured in simulations and the one obtained through the equations differed by an angle corresponding to the width of the spiral on the obstacle boundary. To compensate for this, we add θ_{sw} to ϕ, which is the width of S on the obstacle boundary. In Eq. (5) we took the quantity to the right-hand side (RHS).

Equation (5) is plotted as a function of T_{cp} for an obstacle of radius $r = 4$ for three different phase differences $\alpha = 0, \pi/4$, and $-\pi/4$ in Fig. 4(a). The curve predicted by Eq. (5) agrees with the one obtained through simulations.

What happens when the initial phase difference α is varied? Consider a case with $\alpha = \pi/4$. Then S is much closer to T at $t = 0$. If H has to meet the collision point of T and S simultaneously and unpin the spiral, then the $\boldsymbol{E}$ field should move much faster on the boundary of the obstacle. So it should have a shorter time period, i.e., the cutoff period $T^*_{cp}(\alpha = \pi/4) < T^*_{cp}(\alpha = 0)$. If $\alpha = -\pi/4$ is the initial phase difference then S is closer to H than T at $t = 0$. So S has more distance to cover on the boundary of the obstacle to reach T. So, $\boldsymbol{E}$ should have a longer time period $[T^*_{cp}(\alpha = -\pi/4) > T^*_{cp}(\alpha = 0)]$ such that H reaches the collision point of T and S only when those two collide. So, depending upon how the initial phase difference α is varied, the period of the $\boldsymbol{E}$ field should be timed so that H, S, and T meet together and unpin the spiral. This confirms that in this mechanism of unpinning, we do not have an unpinning window. However, for a given phase difference α, we only have a threshold value for T_{cp} below which there is always unpinning.

The variation of the excitable gap ϕ as a function of T_{cp} for different phase differences (α's) are shown in Fig. 4(a). The x intercept of each curve gives the cutoff period T^*_{cp}. Once the cutoff period T^*_{cp} is determined for an obstacle of radius r and phase difference α, the unpinning is guaranteed for all the time periods lower than T^*_{cp}.

If we set the left-hand side of Eq. (5) to zero, we can write T^*_{cp} as a function of the phase difference α and the obstacle radius r. To test our theory, we performed simulations for obstacles of a different radius and a fixed phase difference of $\alpha = 0$. The curve obtained through simulation study matches the theoretical predictions. The results are shown in Fig. 4(b).

IV. CONCLUSION

In this paper, we identified a robust mechanism for unpinning the spiral waves using a CPEF. We show that for an obstacle of a given radius and fixed phase difference of the spiral, it is always possible to time the period of the electric field so that unpinning is guaranteed. This period is called the cutoff period of the electric field. When the period of the electric field is below the cutoff, the spiral is unpinned before it finishes one full rotation around the obstacle and within the first rotation of the electric field. Our theory accurately predicts this cutoff period and is also quantitatively consistent with all the simulation results. Since arguments used in deriving the theory are based only on fundamental properties of the excitable media, we expect these results to be valid in more general settings.

Typical unpinning studies with field stimulus identify an unpinning window, which is a phase window of the spiral during which it can be unpinned using a field pulse. However, in our mechanism with the CPEF, there is no unpinning window. All rotating fields below the cutoff frequency can result in unpinning. Yet it must be noted that we use a simple monodomain model for simulating the effect of the electric field near the obstacle. A bidomain model, which is the more accurate model of the cardiac tissue, predicts a complicated distribution of polarization around an obstacle, and it could affect the mechanism of unpinning [19].

Our results can be tested in experiments that show 2D excitation waves, including cardiac monolayers and excitable chemical media. Specifically, experimental verification of the results showed in Fig. 2 would serve as a qualitative test for our mechanism. The CPEF can be obtained by using two perpendicular AC electric fields with a phase difference of $\pi/2$ generated with a pair of electrodes kept mutually perpendicular to each other. We hope that our analytical results of the spiral wave unpinning using CPEF will stimulate further studies in this direction.

ACKNOWLEDGMENTS

This article would not be possible without the valuable suggestions of V. Krinsky. TKS thanks the SERB (DST) for funding via early career research grant (ECR/2016/000983). NKA thanks UGC Government of India for financial assistance under the UGC-NET-JRF scheme.

APPENDIX: UNPINNING OF CLOCKWISE ROTATING SPIRAL

The unpinning of a clockwise rotating spiral by $\boldsymbol{E}$ field is shown in Fig. 5. After the $\boldsymbol{E}$ field induces the depolarization, H and S start moving towards each other. They eventually collide and start detaching from the obstacle as the excitation cannot go past the refractory tail left behind by the other [Fig. 5(c)]. Since the $\boldsymbol{E}$ field is rotating, it induces a new excitation head N once it crosses the refractory tail of S. The nonzero excitable gap ϕ from the wavefront of N to the wavefront of T, when H and S just detach from the obstacle, prevents unpinning. In Figs. 5(g) to 5(l) the $\boldsymbol{E}$ field having a smaller rotation period ($T_{cp} = 3.6764$) is used. Now, when H and S fuse and detach from the obstacle, the new head N already collided with T. So, there is no excitable gap. This leads to the successful unpinning of the spiral [see Fig. 5(l)]. Since we kept the radius of the obstacle and phase difference fixed, similar to the anticlockwise case, if we keep on reducing the time period T_{cp}, we will reach a point where the excitable gap $\phi = 0$. This is the cutoff time period T^*_{cp} of the $\boldsymbol{E}$ field. Below this, ϕ is always zero, and therefore there is always unpinning.

The schematic diagram of the clockwise spiral unpinning is shown in Fig. 6. α is the phase difference between the $\boldsymbol{E}$ field and the spiral wavefront at time $t = 0$. At the time t_0, the nucleated wave subtends a symmetric angle of $2\theta_0$. When the depolarization emerges out of the obstacle, S moves clockwise towards H, covering a distance of $v_s t_0$. Later, H and S collide at time $t = t_1$.

The angle covered by H before the collision with S can be given as $\theta_2 = \theta_0 + (2\pi/T_{cp})(t_1 - t_0)$. In the meantime, S travels clockwise and covers an angular distance of $(v_s t_1)/r$. But we have $\theta_2 + (v_s t_1)/r = \pi + \alpha$. We use these conditions to obtain a formula for t_1:

$$t_1 = \left(\pi + \alpha - \theta_0 + \frac{2\pi t_0}{T_{cp}}\right)\left(\frac{r T_{cp}}{2\pi r + T_{cp} v_s}\right). \quad \text{(A1)}$$

Once H and S collide, they begin to detach from the obstacle. As the detachment is in progress, the anticlockwise rotating $\boldsymbol{E}$ field, nucleates a new head N once it crosses the

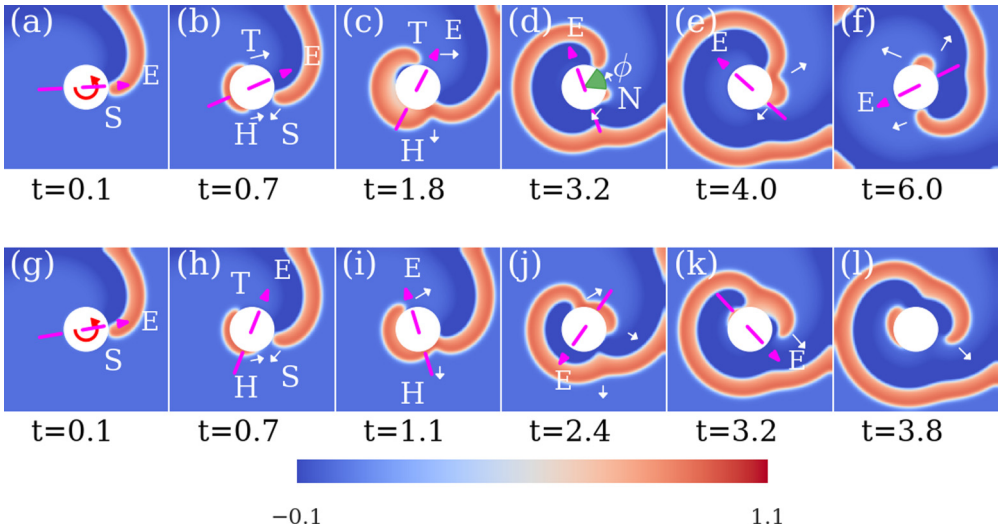

FIG. 5. Unpinning of a clockwise rotating spiral. The radius of the obstacle $r = 4$ and the phase difference $\alpha = 0$. (a)–(d) Unsuccessful case, period of the rotating field $T_{cp} = 10.4166$. (a) A clockwise rotating pinned spiral wave S. (b) Excitation is emitted from the obstacle. (c) H and S collide. (d) When H and S fuse together and detach from the obstacle, the electric field nucleates a new wave N. The excitable gap $\phi > 0$ (shaded in green) between N and T keeps the spiral pinned to the obstacle (f). (g)–(l) Successful case, period of the rotating field, $T_{cp} = 3.6764$. (j) When N collides with T, the excitable gap is zero, and this leads to successful unpinning (l).

refractory tail of S. For an obstacle of a given radius, how fast the $\boldsymbol{E}$ field crosses the refractory tail depends on how small its time period T_{cp} is. Let us denote the time taken by the $\boldsymbol{E}$ field to cross the refractory tail of S and nucleate N as $\Delta\tau_1$. Once the detachment of H and S from the obstacle is complete at time $t = t_1 + \Delta\tau_2$, we measure the excitable gap $\phi = 2\pi - (\theta_N + \theta_T)$. Here, $\Delta\tau_2$ is the time taken by H and S to detach from the obstacle after their collision at $t = t_1$. The angle covered by T can be written as $\theta_T = \theta_0 + (t_1 - t_0 + \Delta\tau_2)(v_T/r)$ whereas the total angle covered by the head (H and N included) is $\theta_N = \theta_0 + (2\pi/T_{cp})(t_1 - t_0) + (2\pi/T_{cp})(\Delta\tau_2 - \Delta\tau_1)$.

We can identify two cases depending on whether the term $(\Delta\tau_2 - \Delta\tau_1)$ in θ_N is positive or negative. The first case is $\Delta\tau_2 > \Delta\tau_1$. Here, T_{cp} is fast enough so that the new head N is nucleated before H and S detaches from the obstacle. Then the excitable gap ϕ can be given as

$$\phi = 2(\pi - \theta_0) - \left(\frac{2\pi}{T_{cp}} + \frac{v_T}{r}\right)(t_1 - t_0 + \Delta\tau_2) + \frac{2\pi\,\Delta\tau_1}{T_{cp}} - \theta_{sw}. \tag{A2}$$

In theory, the angular distance ϕ is calculated between the collision point of H and S and the wavefront of T. But, in simulations, it is measured between the wavefronts of N and T. To compensate for this, we subtract θ_{sw} from Eq. (A2). Here, θ_{sw} is the width of the newly nucleated head N on the boundary of the obstacle.

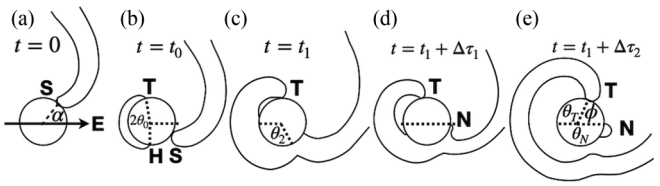

FIG. 6. Schematic diagram of clockwise spiral unpinning. (a) Pinned spiral wave S. α is the phase difference between the $\boldsymbol{E}$ field and the spiral wavefront at time $t = 0$. (b) At $t = t_0$, excitation emerges out symmetrically making an angle θ_0. Meanwhile, S covers a distance of $v_s t_0$ moving clockwise. (c) S and H collide at time t_1. θ_1 and θ_2 are the angle covered by S and H. Meanwhile, T covers a distance of $v_T t_1$. (d) At time $t_1 + \Delta\tau_1$, the rotating electric field nucleates a new wave N after crossing the refractory tail of S. (e) At $t = t_1 + \Delta\tau_2$, H and S detach from the obstacle. The excitable gap $\phi = 2\pi - (\theta_N + \theta_T)$.

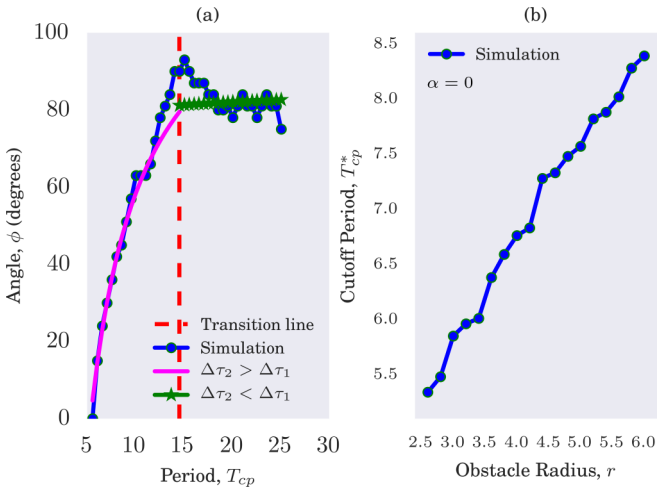

FIG. 7. (a) Graph of the excitable gap ϕ as a function of period of the rotating electric field T_{cp} for a clockwise rotating spiral. The radius of the obstacle $r = 4$ and the phase difference $\alpha = 0$. (b) Graph of cutoff period T^*_{cp} as a function of obstacle radius r for clockwise rotating spiral.

In the second case (i.e., $\Delta\tau_2 < \Delta\tau_1$), T_{cp} is so slow that it cannot cross refractory tail of S until H and S detach from the obstacle. So N does not reappear at all and $\Delta\tau_1 = 0$. So, $\theta_N = \theta_0 + (2\pi/T_{cp})(t_1 - t_0)$. Then, the excitable gap ϕ can be written as

$$\phi = 2(\pi - \theta_0) - \left(\frac{2\pi}{T_{cp}} + \frac{v_T}{r}\right)(t_1 - t_0) - \frac{v_T \Delta\tau_2}{r}. \quad \text{(A3)}$$

In the second case, ϕ is measured from the point of collision between the H and S.

The parameters $\Delta\tau_1$ and $\Delta\tau_2$ are measured directly from the simulations. As mentioned above, $\Delta\tau_1$ varies with the period of the applied E field. For an obstacle of radius r and phase difference α, we measured $\Delta\tau_1$ as a function of T_{cp}. For the measured values, we obtain a straight line fit ($\Delta\tau_1 = mT_{cp} + c$) where m and c are the slope and intercept of the straight line. Both the parameters m and c are the functions of radius r and the spiral phase α. The measured values of the parameter $\Delta\tau_2$ are found to be a constant.

Somewhere in between the two cases $\Delta\tau_2 = \Delta\tau_1$. We call the corresponding T_{cp} as T_{cp} transition. Since $\Delta\tau_2$ is a known constant, the value of T_{cp} transition can be calculated from the straight line fit of $\Delta\tau_1$. The results are summarized in Fig. 7. Similar to the anticlockwise mechanism, the unpinning happens within one rotation of the $\boldsymbol{E}$ field, and if we vary the phase difference α, we find that there is no unpinning window for this mechanism.

[1] M. A. Dahlem and S. C. Müller, Ann. Phys. (Berl.) **13**, 442 (2004).

[2] S. J. Schiff, X. Huang, and J.-Y. Wu, BMC Neurosci. **8**, P61 (2007).

[3] J. M. Davidenko, A. V. Pertsov, R. Salomonsz, W. Baxter, and J. Jalife, Nature **355**, 349 (1992).

[4] M. E. Josephson, S. R. Spielman, A. M. Greenspan, and L. N. Horowitz, Am. J. Cardiol. **44**, 623 (1979).

[5] P. Bittihn, A. Squires, G. Luther, E. Bodenschatz, V. Krinsky, U. Parlitz, and S. Luther, Philos. Trans. R. Soc. A **368**, 2221 (2010).

[6] A. Pumir and V. Krinsky, J. Theor. Biol. **199**, 311 (1999).

[7] T. Shajahan, S. Berg, S. Luther, V. Krinski, and P. Bittihn, New J. Phys. **18**, 043012 (2016).

[8] S. Punacha, S. Berg, A. Sebastian, V. Krinski, S. Luther, and T. Shajahan, Proc. R. Soc. A **475**, 20190420 (2019).

[9] R. A. Gray and J. P. Wikswo, Nature **475**, 181 (2011).

[10] J.-X. Chen, H. Zhang, and Y.-Q. Li, J. Chem. Phys. **124**, 014505 (2006).

[11] X. Feng, X. Gao, D.-B. Pan, B.-W. Li, and H. Zhang, Sci. Rep. **4**, 4831 (2014).

[12] X. Feng, X. Gao, J.-M. Tang, J.-T. Pan, and H. Zhang, Sci. Rep. **5**, 13349 (2015).

[13] X. Feng and X. Gao, Nonlinear Dyn. **98**, 1919 (2019).

[14] L. Ji, Y. Zhou, Q. Li, C. Qiao, and Q. Ouyang, Phys. Rev. E **88**, 042919 (2013).

[15] A. Pumir, V. Nikolski, M. Hörning, A. Isomura, K. Agladze, K. Yoshikawa, R. Gilmour, E. Bodenschatz, and V. Krinsky, Phys. Rev. Lett. **99**, 208101 (2007).

[16] D.-B. Pan, X. Gao, X. Feng, J.-T. Pan, and H. Zhang, Sci. Rep. **6**, 1 (2016).

[17] P. Bittihn, M. Hörning, and S. Luther, Phys. Rev. Lett. **109**, 118106 (2012).

[18] F. H. Fenton, E. M. Cherry, A. Karma, and W.-J. Rappel, Chaos **15**, 013502 (2005).

[19] S. Takagi, A. Pumir, D. Pazo, I. Efimov, V. Nikolski, and V. Krinsky, Phys. Rev. Lett. **93**, 058101 (2004).